Optics Letters

Steering optical comb frequencies by rotating the polarization state

Yanyan Zhang,[1,2] Xiaofei Zhang,[1,2] Lulu Yan,[1,2] Pan Zhang,[1] Bingjie Rao,[1] Wei Han,[1,2] Wenge Guo,[1] Shougang Zhang,[1,2] and Haifeng Jiang[1,2,*]

[1]Key Laboratory of Time and Frequency Primary Standards, National Time Service Center, Chinese Academy of Sciences, Xi'an 710600, China
[2]School of Astronomy and Space Science, University of Chinese Academy of Sciences, Beijing 100049, China
*Corresponding author: haifeng.jiang@ntsc.ac.cn

Received 30 October 2017; accepted 9 November 2017; posted 13 November 2017 (Doc. ID 310117); published 8 December 2017

We demonstrate a new approach to steer the frequencies of a nonlinear polarization-rotation mode-locked laser, where a specially designed intrcavity electro-optic modulator tunes the polarization state of the laser signal. This approach not only results in the broadband associated with high performance, but also results in a large dynamic range associated with good robustness. Our experimental results show that frequency control dynamic ranges are at least one order of magnitude larger than those of the previous ultra-fast frequency control techniques, reaching hundreds of hertz and hundreds of megahertz for repetition rate (f_r) and carrier-envelope-offset frequency (f_{ceo}), respectively.

OCIS codes: (140.3518) Lasers, frequency modulated; (120.4570) Optical design of instruments; (140.4050) Mode-locked lasers.

https://doi.org/10.1364/OL.42.005145

Optical frequency combs, which establish the bridge between the microwave domain and the optical one, enable the precise measurement of optical signals in phase and have revolutionized a wide range of fields such as fine optical spectroscopy [1], optical frequency standards [2], ultra-fast science research [3], ultra-stable microwave generation [4], and precise ranging measurement [5]. To a great extent, all the above-mentioned applications are based on the precise control of the repetition rate (f_r) and carrier-envelope-offset frequency (f_{ceo}).

Generally, the capability of frequency control is determined by two main aspects: the servo bandwidth associated with performance and the dynamic range associated with robustness. The f_r is usually controlled using a piezoelectric transducer (PZT) with a few tens of kilohertz bandwidth limited by acoustic resonances [6]. Bandwidths over 100 kHz are possible by using two PZT: a slower PZT with a large modulated range and a faster PZT with high resonance frequency [7,8]. High bandwidths (up to 1 MHz) are obtained using an intracavity electro-optic modulator (EOM) by tuning the optical length of the cavity [9–11]. More specifically, a waveguide EOM is employed with an extremely high bandwidth of more than 1 MHz and low drive voltages [12,13]. Unfortunately, the EOM produces a small control range of the f_r by changing the refractive index of the EO crystal. It is a common strategy to combine an EOM and a low-bandwidth PZT, achieving tight stabilization of the f_r over a large dynamic range, which needs a complex control technique [14]. The f_{ceo} is typically controlled by tuning the pumping power with a relatively low bandwidth (100 kHz typically) limited by the gain lifetime [15,16]. Alternatively, an extracavity acousto-optic modulator is used for f_{ceo} control with the submegahertz bandwidth [17,18], though the method has a limitation of the output power and the diffraction effect on the laser; megahertz bandwidth (over 1 MHz) is documented by using a graphene modulator (GM), which modulates the intracavity laser power without adverse effects on the laser [19,20]. However, another feedback to the pump power for long-term operation has to be adopted at the same time due to the small dynamic range of the GM.

In a fiber-based nonlinear polarization-rotation (NPR) system, the laser keeps a mode-locked state, while the polarization state changes over a certain controlled dynamic range of comb frequencies [21,22]. This range corresponds to a controlled dynamic range of comb frequencies. In this Letter, we stabilize frequencies of an optical comb by tuning the polarization state with a specially designed intracavity EOM. The preliminary results show that this approach not only has broadband frequency control ability such as what is in a traditional intracavity EOM technique, but also significantly enlarges the control dynamic range.

The experimental setup is shown in Fig. 1. The mode-locked laser, pumped with two 980 nm 500 mW pigtailed diode lasers, has a repetition rate of 192 MHz. The output power is ~144 mW. The peak power wavelength is 1575 nm, and the full width at half-maximum of the spectrum is ~30 nm. The ring cavity of the laser includes three types of fibers: a 41 cm (Er110-4/125) erbium-doped fiber, a 48 cm single-mode fiber (SMF)-28 fiber, and a 5 cm HI1060 fiber. The PZT (0.5 cm) driven by a tunable high-voltage signal generator (0 V, +150 V) tunes the reflection mirror over a range of ~5 μm, which corresponds to a shift in the repetition rate of ~1 kHz. A specially designed 3 mm thick EOM is used

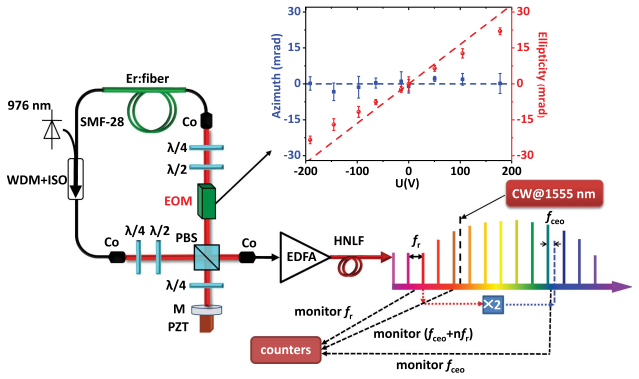

Fig. 1. Experimental setup. The Er:fiber femtosecond laser source has a ring cavity, including four wave plates, a PBS, three collimators (Cos), a wavelength division multiplexer (WDM) with an isolator (ISO), an EOM, and fibers. A PZT mounted on a mirror (M) is employed to adjust the cavity length. A highly nonlinear fiber (HNLF) and an erbium-doped fiber amplifier (EDFA) produce the f_{ceo} signal. Three frequency counters record the shifts of f_r, f_{ceo}, and the comb teeth at 1555 nm. The inset shows the polarization state shift in ellipticity (theoretical data, red dashed line; experimental data, red points) and azimuth (theoretical data, blue dashed line; experimental data, blue point) as a function of voltage on the EOM.

to control the polarization state. The EOM, inserted right after the polarization beam splitter (PBS), is driven with a high-voltage signal generator (−200, +200 V) with a modulation port for response measurement and stabilization of the comb frequencies. The f_r, f_{ceo}, and the frequency of the mode near the reference laser (1555 nm) are monitored using frequency counters.

The EOM is employed to tune the polarization state with a coefficient of ∼0.12 mrad/V, which is measured over the range from -200 to 200 V. It is made of an $LiNbO_3$ crystal with a size of $3(x) \times 5(y) \times 3(z)$ mm^3. The direction of the laser passes along the crystal's optical axis (defined as the z-axis). The external electric field is parallel to the x-axis, and the two yz surfaces are coated with gold. The incidence light has a linear polarization state aligned to the x-axis.

The rotation of the polarization induced by the external electric field can be calculated using the refractive index ellipsoid theory [23]. The phase change between the x-axis and y-axis of the incident light is given by

$$\Delta\varphi = (2\pi/\lambda) L r_{22} V n_0^3 / d, \tag{1}$$

where r_{22} is the nonzero component of the electro-optic tensor for $LiNbO_3$, n_0 is the index of refraction of $LiNbO_3$ crystal, V is the voltage applied across the EOM, and d is the distance between the electrodes on the EOM. By using the Jones matrix and stokes vectors [24,25], we can express the polarization rotation in azimuth and in ellipticity as

$$\tan 2\psi = \tan 2\theta / \cos\varphi,$$
$$\sin 2\chi = \cos 2\theta \sin\varphi, \tag{2}$$

where ψ is the azimuth angle, χ is the ellipticity angle, and θ is the angle between the initial polarization direction and x-axis. In this case, the polarization of the incident light is perpendicular to the x-axis ($\theta = 0$). As shown in the inset of Fig. 1, the theoretical rotation of the polarization in ellipticity and in azimuth are 0.14 mrad/V and null, respectively, which is in agreement with the experimental result of 0.12 mrad/V.

Figure 2 shows the measure date for the response of comb frequencies to the voltage applied on the EOM. The frequency variation of a comb tooth @1555 nm ($nf_r + f_{ceo}$), f_{ceo}, and nf_r as a function of voltage gives corresponding coefficients of about 0.07 MHz/V, −0.33 MHz/V, and 0.40 MHz/V. The control coefficient of f_r, in contrast to the traditional intracavity EOM technique with the same size of EOM, is about one order of magnitude lager [26]. Note that our EOM modulates f_{ceo} and nf_r by almost the same amount, indicating that it can work as a modulator for either f_r or f_{ceo}. Furthermore, we observe that the frequency of the comb tooth is relatively stable, resulting in smaller crosstalk between the control servo loops of f_{ceo} and the tooth's frequency. On the other hand, the sensitivity of f_r to the pump current is about 7 MHz/mA, while that of the f_{ceo} is about 0.5 MHz/mA and is 10 times smaller than the modulation of f_r; such a relation between polarization and current can easily control the comb's frequency stabilization. Another advantage of this approach is that the power fluctuation introduced by the f_{ceo} control is small, about 1/270th of the pumping power method in Ref. [26]. This is good for frequency comb utilization because some applications are sensitive to power variation.

To estimate the frequency steering range by tuning the polarization, we change the ellipticity χ and azimuth ψ by rotating the wave plates following the EOM. The tuning range of the ellipticity χ and azimuth ψ are 0.24 and 0.28 rad, respectively, as shown in Fig. 3. Beyond this range, the signal-to-noise ratio of f_{ceo} starts to drop down and/or a continuous-wave (CW) signal appears in an optical spectrum. The dynamic ranges of f_r and f_{ceo} are about 1 kHz and 850 MHz over this range. These ranges are comparable to those commonly used in large dynamic frequency control techniques (i.e., f_r controlled with a PZT and f_{ceo} controlled by tuning the pumping power), implying that it can be used to steer the optical comb frequencies with both a broad bandwidth and a relatively large dynamic range.

In Fig. 3(a), all the measured points are distributed in a tilt plane, where the sensitivities of f_r are ∼3 kHz/rad in ellipticity

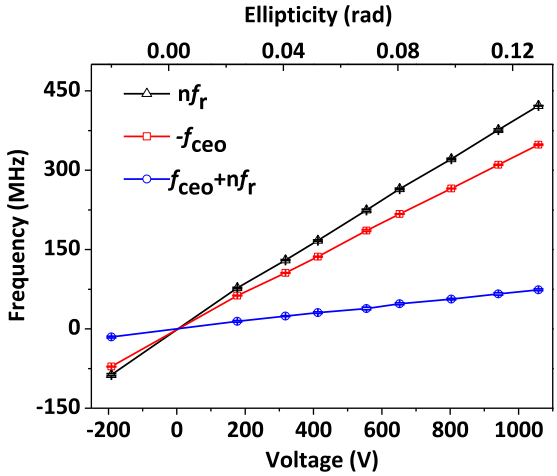

Fig. 2. Variation of comb frequencies versus voltage acting on the intracavity EOM. Frequency variations of the comb teeth @1555 nm (nf_r, $+f_{ceo}$), f_{ceo}, and nf_r are shown with blue, red, and black lines, respectively, where n is about 1×10^6.

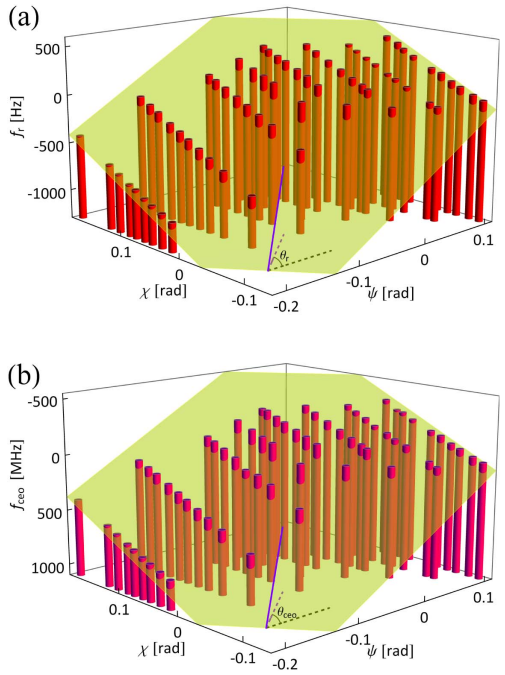

Fig. 3. Relation between comb frequencies and polarization state. (a) Variation of repetition rate f_r as a function of ellipticity χ and azimuth ψ. (b) Variation of the carrier-envelope-offset frequency f_{ceo} as a function of ellipticity χ and azimuth ψ. The maximum directions, denoted by Θ_r and Θ_{ceo}, are 0.68 and 0.67 rad, respectively, measured from the azimuth axis, so that one can control the frequencies with maximum sensitivities of ~6 kHz/rad and -5000 MHz/rad, respectively.

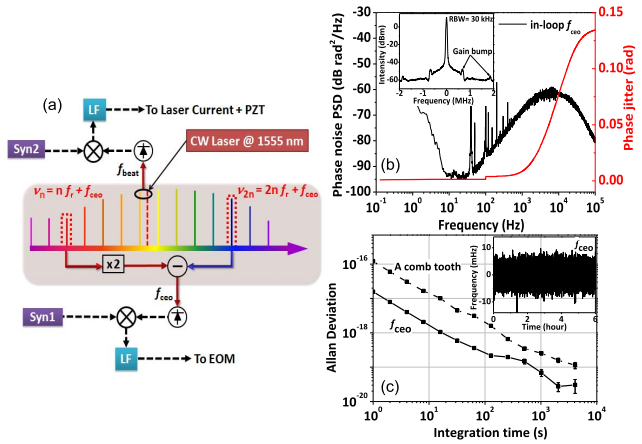

Fig. 4. Setup and results of comb frequency stabilization. (a) Schematic of the comb's frequency stabilization, where f_{ceo} is phase-locked onto a synthesizer (Syn1) with the new technique, and the comb teeth (~193 THz) are phase-locked onto a CW laser (1555 nm) with a frequency shift produced by a second synthesizer (Syn2). Loop filters (LFs) are proportional-integral amplifiers. (b) In-loop phase noise of f_{ceo}; the inset shows the spectrum. (c) In-loop relative frequency instability of f_{ceo} (solid black square) and a comb tooth (dashed black square); the inset shows the raw data of f_{ceo} fluctuations.

and ~5 kHz/rad in azimuth, exhibiting a maximum sensitivity at ~6 kHz/rad. In Fig. 3(b), the sensitivities of f_{ceo} are about −2700 MHz/rad in ellipticity and about −4200 MHz/rad in azimuth, exhibiting a maximum sensitivity of about −5000 MHz/rad. It is clear that the tilt plates in both subfigures are very similar, showing that the comb teeth at 1.5 μm (i.e., $f_{ceo} + nf_r$) are relatively stable. Such behavior can be understood as related to the birefringence effect of a laser cavity. A change of power ratio between slow and fast axes accompanied with polarization state changes leads to a group-velocity shift. Thus, the phase velocity, dominated by gain and nonlinear effects is relatively stable. Consequently, f_{ceo}, representing the difference between the group velocity and phase velocity, is also sensitive to polarization state. Furthermore, the dynamic range of frequency control causing by the cavity's birefringence can be calculated through the following method: first, we assume that all birefringence is attributed to the Er110 fiber because the birefringence coefficients of the SMF-28 fiber and the HI1060 fiber are small and can be neglected; then the birefringence coefficient of the Er110 is calculated (about 670 fs/m) according to the character of the optical spectrum in Ref. [27]. Finally, we can deduce that the birefringence level of our experimental system is ~320 fs, which induces a relative shift of the repetition rate of $\sim 6.2 \times 10^{-5}$, corresponding to a maximum sensitivity of 12 kHz/rad. Compared with the experimental one, the reduction factor of 0.5 is attributed to the fact that the polarization state rotation is not along with the maximum efficient direction.

To verify frequency steering ability of our approach, we stabilize f_{ceo} onto an frequency reference with the EOM and simultaneously stabilize the comb teeth onto a CW laser at 1555 nm by controlling the pumping power and the PZT, as shown in Fig. 4(a). The phase noise of f_{ceo} is below −60 dB/rad²/Hz, except for some noise bumps near 100 Hz, as shown in Fig. 4(b). The phase jitter from 1 Hz to 100 kHz is about 0.1 rad. The gain bumps show up at ~650 kHz and ~1.8 MHz [see the inset of Fig. 4(b)]; the former one is attributed to the integral gain, while the latter one is due to the proportional gain, corresponding to the control bandwidth of f_{ceo}. The peak in-loop frequency jitter, recorded with a frequency counter, is well below 10 mHz at a 1 s gate time, as shown the inset of Fig. 4(c). The frequency stability normalized by 193 THz (1555 nm) is about $2 \times 10^{-17}/\text{s}$ and scales down with a slope of $1/\tau$ for short terms, as shown in Fig. 4(c). Note that the frequency counters used are Π-type ones made by K & K company under an averaging mode.

The relative frequency stability of a comb tooth is about 10 times higher because the response speed of the pumping power control is relatively slow. The crosstalk effect between the two frequency control loops cannot be observed, even under high gain conditions; yet, it was the dominating limitation of our previous system with the traditional intracavity EOM technique [26].

This technique can also be used for frequency stabilization of f_r. We phase-lock the 48th repetition frequency harmonic to a 9.2 GHz reference signal using the EOM. The in-loop relative frequency instability of f_r is $8 \times 10^{-15}/\text{s}$, limited by the noise floor of the measurement system.

In summary, we have developed a new technique for the control of optical comb frequencies by tuning the polarization state of the laser. This approach can steer frequencies in a broad bandwidth and over a large dynamic range by taking advantage of the birefringence of the whole laser cavity. With this technique, hybrid frequency control is no longer mandatory for tight stabilization of the comb frequency [14]. In addition,

it exhibits fewer side effects such as small crosstalk and small power variation during frequency control. Moreover, improving the frequency control coefficient can be easily accomplished by employing high birefringence fibers.

Funding. National Natural Science Foundation of China (NSFC) (11775253, 91336101, 91536217); Youth Innovation Promotion Association of the Chinese Academy of Sciences (2015334); Chinese Academy of Sciences (CAS) (West Light Foundation 2013ZD02).

REFERENCES

1. S. A. Diddams, L. Hollberg, and V. Mbele, Nature **445**, 627 (2007).
2. B. J. Bloom, T. L. Nicholson, J. R. Williams, S. L. Campbell, M. Bishof, X. Zhang, W. Zhang, S. L. Bromley, and J. Ye, Nature **506**, 71 (2014).
3. A. Wirth, M. T. Hassan, I. Grguraš, J. Gagnon, A. Moulet, T. T. Luu, S. Pabst, R. Santra, Z. A. Alahmed, A. M. Azzeer, V. S. Yakovlev, V. Pervak, F. Krausz, and E. Goulielmakis, Science **334**, 195 (2011).
4. J. J. Mcferran, E. N. Ivanov, A. Bartels, G. Wilpers, C. W. Oates, S. A. Diddams, and L. Hollberg, Electron. Lett. **41**, 650 (2005).
5. I. Coddington, W. C. Swann, L. Nenadovic, and N. R. Newbury, Nat. Photonics **3**, 351 (2009).
6. B. R. Washburn, S. A. Diddams, and N. R. Newbury, Opt. Lett. **29**, 250 (2004).
7. T. R. Schibli, I. Hartl, D. C. Yost, M. J. Martin, A. Marcinkevičius, M. E. Fermann, and J. Ye, Nat. Photonics **2**, 355 (2008).
8. A. Ruehl, A. Marcinkevicius, M. E. Fermann, and I. Hartl, Opt. Lett. **35**, 3015 (2010).
9. D. D. Hudson, K. W. Holman, R. J. Jones, S. T. Cundiff, and J. Ye, Opt. Lett. **30**, 2948 (2005).
10. C. Benko, A. Ruehl, M. J. Martin, K. S. E. Eikema, M. E. Fermann, I. Hartl, and J. Ye, Opt. Lett. **37**, 2196 (2012).
11. D. Nicolodi, B. Argence, W. Zhang, R. L. Targat, G. Santarelli, and Y. L. Coq, Nat. Photonics **8**, 219 (2014).
12. Y. Iwakuni, H. Inaba, Y. Nakajima, T. Kobayashi, K. Hosaka, A. Onae, and F. L. Hong, Opt. Express **20**, 13769 (2012).
13. E. Baumann, F. R. Giorgetta, J. W. Nicholson, W. C. Swann, I. Coddington, and N. R. Newbury, Opt. Lett. **34**, 638 (2009).
14. S. Droste, G. Ycas, B. R. Washburn, I. Coddington, and N. R. Newbury, Nanophotonics **5**, 196 (2016).
15. J. J. Mcferran, W. C. Swann, B. R. Washburn, and N. R. Newbury, Appl. Phys. B **86**, 219 (2007).
16. I. Hartl, L. Dong, M. E. Fermann, T. R. Schibli, A. Onae, F. L. Hong, H. Inaba, K. Minoshima, and H. Matsumoto, *Optical Fiber Communication Conference (OFC)* (2005).
17. R. J. Jones and J. C. Diels, Phys. Rev. Lett. **86**, 3288 (2001).
18. S. Koke, C. Grebing, H. Frei, A. Anderson, A. Assion, and G. Steinmeyer, Nat. Photonics **4**, 462 (2010).
19. C. C. Lee, C. Mohr, J. Bethge, S. Suzuki, M. E. Fermann, I. Hartl, and T. R. Schibli, Opt. Lett. **37**, 3084 (2012).
20. N. Kuse, C. C. Lee, J. Jiang, C. Mohr, T. R. Schibli, and M. E. Fermann, Opt. Express **23**, 24342 (2015).
21. A. D. Kim, J. N. Kutz, and D. J. Muraki, IEEE J. Quantum Electron. **36**, 465 (2000).
22. N. R. Newbury and B. R. Washburn, IEEE J. Quantum Electron. **41**, 1388 (2005).
23. D. F. Nelson, J. Opt. Soc. Am. **65**, 1144 (1975).
24. M. Nakazawa, K. Kikuchi, and T. Miyazaki, *High Spectral Density Optical Communication Technologies* (Springer, 2007).
25. W. F. Rong, L. Dupont, Y. X. Wang, Y. K. Yeo, J. Chen, W. Kuang, and V. Paulose, IEEE Photon. J. **2**, 865 (2010).
26. L. L. Yan, Y. Y. Zhang, L. Zhang, S. T. Fan, X. F. Zhang, W. G. Guo, S. G. Zhang, and H. F. Jiang, Chin. Phys. Lett. **32**, 104207 (2015).
27. Y. Y. Zhang, S. T. Fan, L. L. Yan, L. Zhang, X. F. Zhang, W. G. Guo, S. G. Zhang, and H. F. Jiang, Opt. Express **25**, 21719 (2017).